

tapered area of the junction. The phase-front accelerator regions effectively act as asymmetric power dividers between the central branch and the side branches, thus allowing a certain portion of the incoming energy to propagate along the three branches. By varying the positions of the tips (i.e. d_1 and d_2) and the areas of the shaded regions (i.e. between angles θ_1 and θ_2), the power distribution of the output branches can be controlled. As the shaded region also has a refractive index n_2 which is slightly lower than that of the cladding, n_0 ,⁴ the phase front of the modal fields will be channelled into their corresponding branches without causing significant modal mismatch.⁵

Results and discussion: To demonstrate the operation of the proposed optical branching circuit design, the beam-propagation method (BPM) was employed for the numerical simulation. The waveguides are assumed to operate in single-mode TE₀ and the refractive index parameters are chosen as $n_0 = 1.5$, $n_1 = 1.502$ and $n_2 = 1.498$. The operating wavelength is $1 \mu\text{m}$, the angle between the adjacent branches θ_0 is $1/100$ rad and the phase-front accelerator region is optimised by choosing $\theta_1 = 1/125$ rad and $\theta_2 = 1/630$ rad. The position locations of the tips of the phase-front accelerator regions are set at $d_1 = 0$ and $d_2 = 1.2 \mu\text{m}$.

Figs. 2a and b show, respectively, the amplitude plots of the propagating beam in a conventional structure and our proposed 1×3 optical branching circuit design. It can be

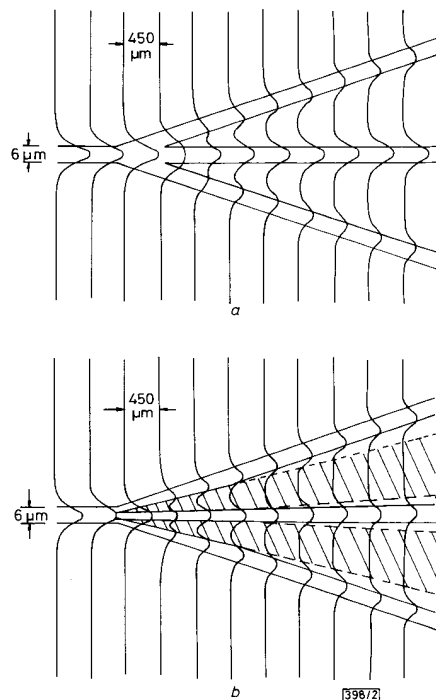


Fig. 2 Amplitude distribution for propagating beam in 1×3 branching circuit

a Conventional structure
b Proposed design

Refractive indices are $n_0 = 1.5$, $n_1 = 1.502$ and $n_2 = 1.498$

observed that the distributed power at the central branch in Fig. 2b is reduced (compared to Fig. 2a) while the power at the side branches is increased. The result shows that the proposed design structure will redistribute the modal power for the three branches instead of attenuating the energy in the central branch.¹ The relative power output ratio of the three branches in Fig. 2a is 0.27:1:0.27, while that in Fig. 2b is 0.99:1:0.99.

1366

Acknowledgment: One of the authors (W. Y. Hung) would like to thank the Sir Edward Youde Foundation for a Memorial Fellowship.

W. Y. HUNG
H. P. CHAN
P. S. CHUNG

5th September 1988

Department of Electronics
Chinese University of Hong Kong
Shatin, New Territories, Hong Kong

References

- 1 BELANGER, M., YIP, G. L., and HARUNA, M.: 'Passive planar multi-branch optical power divider: some design considerations', *Appl. Opt.*, 1983, **22**, pp. 2383-2389
- 2 BECKER, R. A., and JOHNSON, L. M.: 'Low-loss multiple-branching circuits in Ti-indiffused LiNbO₃ channel waveguides', *Opt. Lett.*, 1984, **9**, pp. 246-248
- 3 HARUNA, M., BELANGER, M., and YIP, G. L.: 'Passive 3-branch optical power divider by K⁺-ion exchange in glass', *Electron. Lett.*, 1985, **21**, pp. 533-536
- 4 HUNG, W. Y., CHAN, H. P., and CHUNG, P. S.: 'Novel design of wide-angle single-mode symmetric Y-junctions', *ibid.*, 1988, **24**, pp. 1184-1185
- 5 SHIINA, T., SHIRASHI, K., and KAWAKAMI, S.: 'Waveguide-bend configuration with low-loss characteristics', *Opt. Lett.*, 1986, **11**, pp. 736-738

GENERATION OF 1180 Å PERIOD GRATINGS WITH A Xe ION LASER

Indexing terms: Semiconductor lasers, Lithography, Optoelectronics

Holographic lithography with the 2315 Å line of a xenon ion laser is used to produce gratings in polymethylmethacrylate. An 1180 Å period grating is made and examined with a scanning electron microscope (SEM). This grating period is appropriate for use as a first-order grating with a GaAs distributed feedback laser.

The use of diffraction gratings in optoelectronic devices, such as distributed feedback lasers and distributed Bragg reflectors,¹ requires lithographic techniques capable of generating patterns with a feature size of a few thousand angstroms. Lithographic patterns on this and smaller scales are also required for the fabrication of structures showing quantum size effects such as quantum wires² and quantum boxes.³ The generation of such fine patterns is generally accomplished either by electron beam lithography or by holographic lithography. In this letter we report on the fabrication of 1180 Å period gratings in polymethylmethacrylate (PMMA) using the 2315 Å line of a Xe ion laser and a conventional holographic exposure set-up. In such a set-up the period of the grating is given by

$$d = \frac{\lambda}{n(\sin \alpha - \sin \beta)} \quad (1)$$

where α and β are the angles of incidence of the two beams, n is the index of refraction and λ is the wavelength of the light. The shortest period, $d = \lambda/2n$, is obtained for $\alpha = -\beta = \pi/2$. To reduce d , one can use a high-index prism⁴ or a shorter-wavelength source. Unfortunately, coherent deep UV sources are not abundant. One approach is the generation of deep UV radiation as a harmonic of a powerful, lower-frequency source.⁵

The interference patterns were recorded on GaAs substrates which were spin-coated with a 1% solution of molecular weight 496 K PMMA at 5000 rev/min and prebaked at 170°C for 1 h. Although usually used for electron beam lithography,

PMMA has been shown to be sensitive to ultraviolet radiation with wavelengths of 2500 Å and shorter.⁶ In this region of the spectrum, the Novolac resists have a high absorption coefficient and a low bleachability, making them unsuitable. After exposure, the samples were developed in methyl-isobutylketone (MIBK) for 60 s, rinsed sequentially in isopropanol and water, and blown dry with nitrogen. The samples were sputter-coated with approximately 50 Å of Au/Pd to prevent distortion of the images due to charging during observation by SEM.

Exposure of the PMMA was made with the 2315 Å line of ionised xenon. This ultraviolet transition was first observed by Marling;⁷ the energy level assignments are unknown, but the transition is usually attributed to doubly or triply ionised xenon, Xe III or Xe IV. A simple air-cooled, fused silica discharge tube of 5 mm inner diameter and 60 cm long with ordinary fused silica Brewster's angle windows was used. A 10 nF capacitor charged to 10–20 kV was switched with a 5C22 thyratron to give 0.5 µs, 800 A discharge current pulses at about 40 pulses/s. A pair of mirrors peaked at 2310 Å obtained from Acton Research Corporation provided the optical cavity: a 98% reflecting 2 m spherical mirror and a 97% reflecting flat with 2% transmission. Lasing occurred for the second half of the current pulse, giving triangular pulses 0.25 µs at the base. Average multimode output power was measured with an Eppy thermopile at about 130 µW, giving a peak power of about 25 W with a duty cycle of 10^{-5} . An intracavity aperture was used to select TEM₀₀ operation, with an estimated average intensity of 1.5 mW/cm² at the centre of the Gaussian. Since this particular laser transition exhibited optimum xenon pressures of 5 mtorr or less, gas clean-up by the discharge was relatively rapid; stable operation was obtained for about an hour at a time between gas refills. Because the power drifted somewhat during the exposure, the estimates of total energy deposition are approximate. If we assume that the ratio of the power in the two beams was 2:1 and we account for geometrical factors, the maximum intensity at the PMMA surface was 0.37 times that at the centre of the Gaussian. This gives an intensity of 0.56 mW/cm² in the centre of the exposed regions. Exposure times of 2–10 min were used, with about 5 min giving the best results. A 5 min exposure at 0.56 mW/cm² corresponds to an energy deposition of 0.17 J/cm². This estimate is considered to be good to within a factor of two.

Fig. 1 shows an SEM micrograph of a 1180 Å period grating in the exposed PMMA. This is close to the shortest

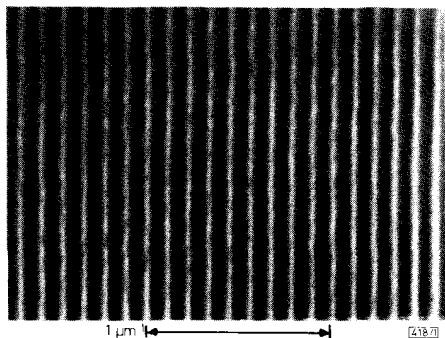


Fig. 1 SEM micrograph of 1180 Å period grating in PMMA

Pattern was generated holographically with 2315 Å emission from a Xe ion laser

period attainable with this laser without the use of a prism to shorten the wavelength. The flatness of the region between the stripes indicates that the exposure reaches the substrate. The grating pattern extends over an area of approximately 1 mm², which corresponds to over 50% of the exposed area. Similar exposures were performed on a thin film of AZ1400 series resist, a Novolac resist, but the resulting resist profiles were poor and did not extend to the substrate.

In conclusion, a new source has been employed for deep UV holographic lithography and it has been shown to be capable of producing features as small as 600 Å. A grating was

produced with a period appropriate for use as a first-order grating for a GaAs/AlGaAs distributed feedback laser. This technique may also be useful in the fabrication of quantum-confined structures such as quantum wires and quantum boxes. The Xe ion laser, although not commercially available, can be assembled in the laboratory as an inexpensive UV source for lithographic purposes.

H. A. ZAREM
M. E. HOENK
W. B. BRIDGES
K. VAHALA
A. YARIV

Department of Applied Physics, 128-95
California Institute of Technology
Pasadena, CA 91125, USA

14th September 1988

References

- 1 YARIV, A.: 'Optical electronics' (Holt, Rinehart & Winston, NY, 1985)
- 2 CIBERT, J., PETROFF, P. M., DOLAN, G. J., GOSSARD, A. C., and ENGLISH, J. H.: 'Optically detected carrier confinement to one and zero dimension in GaAs quantum well wires and boxes', *Appl. Phys. Lett.*, 1986, **49**, pp. 1275–1277
- 3 REED, M. A., RANDALL, J. N., AGGARWAL, R. J., MATYI, R. J., MOORE, T. M., and WETSEL, A. E.: 'Observation of discrete electronic states in a zero-dimensional semiconductor nanostructure', *Phys. Rev. Lett.*, 1988, **60**, pp. 535–537
- 4 YEN, H. W., NAKAMURA, M., GARMIRE, E., SOMEKH, S., and YARIV, A.: 'Optically pumped GaAs waveguide lasers with a fundamental 0.11 µm corrugation feedback', *Opt. Commun.*, 1973, **9**, pp. 35–37
- 5 BJORKLUND, G. C., HARRIS, S. E., and YOUNG, J. F.: 'Vacuum ultraviolet holography', *Appl. Phys. Lett.*, 1974, **25**, pp. 451–452
- 6 LIN, B. J.: 'Deep UV lithography', *J. Vac. Sci. & Technol.*, 1975, **12**, pp. 1317–1320
- 7 MARLING, J. B.: 'Ultraviolet ion laser performance and spectroscopy—Part I: New strong noble-gas transitions below 2500 Å', *IEEE J. Quantum Electron.*, 1975, **QE-11**, pp. 822–834

HARDWARE FADING SIMULATOR FOR A NUMBER OF NARROWBAND CHANNELS WITH CONTROLLABLE MUTUAL CORRELATION

Indexing terms: Telecommunications, Mobile radio systems, Correlation, Data transmission

A multipath fading simulator with a number of narrowband channels with controllable mutual correlation is described. With this simulator it is possible to test the influence of joint fading statistics of mutually correlated channels on a mobile data communication link with frequency diversity.

Simulator principle: One of the methods for mobile data transmission systems to combat multipath fading is frequency diversity. The different diversity channels serving one mobile terminal cannot be considered completely uncorrelated in all cases. Their mutual correlation depends on the mutual frequency separation. Therefore, to test the robustness against multipath fading of mobile data transmission systems with frequency diversity, a radio channel simulator with the possibility of mutual correlation of fading on different channels is desirable.

The bandwidth of the diversity channels is so small (e.g. 25 kHz) that they each can be assumed to encounter flat Rayleigh fading.¹ A single wideband simulator could be used for the simulation of correlated flat-fading channels.² A much simpler and less expensive solution, however, is to assign a separate flat-fading simulator to each channel, and to make adjacent channels correlated. By adjusting the mutual correlations, diversity solutions corresponding to different channel spacings can be tested.